

## Electronic Supplementary Information

### Free-Standing 3D Polyaniline-CNTs Nanocomposite Electrodes for High-Performance Supercapacitors

Yuan Li,<sup>a</sup> Yuzhu Fang,<sup>a</sup> Hong Liu,<sup>b</sup> Xiaoming Wu,<sup>b</sup> and Yong Lu<sup>\*a</sup>

<sup>a</sup> Shanghai Key Laboratory of Green Chemistry and Chemical Processes, Department of Chemistry,

East China Normal University, Shanghai 200062, China

<sup>b</sup> TANTZ Environmental Protection Technologies Ltd., 189 South Dunhe Road,

Guangzhou 510300, China

**\* To whom correspondence should be addressed**

**Fax:** (+86)21-62233424, **E-mail:** ylu@chem.ecnu.edu.cn (Y. Lu.)

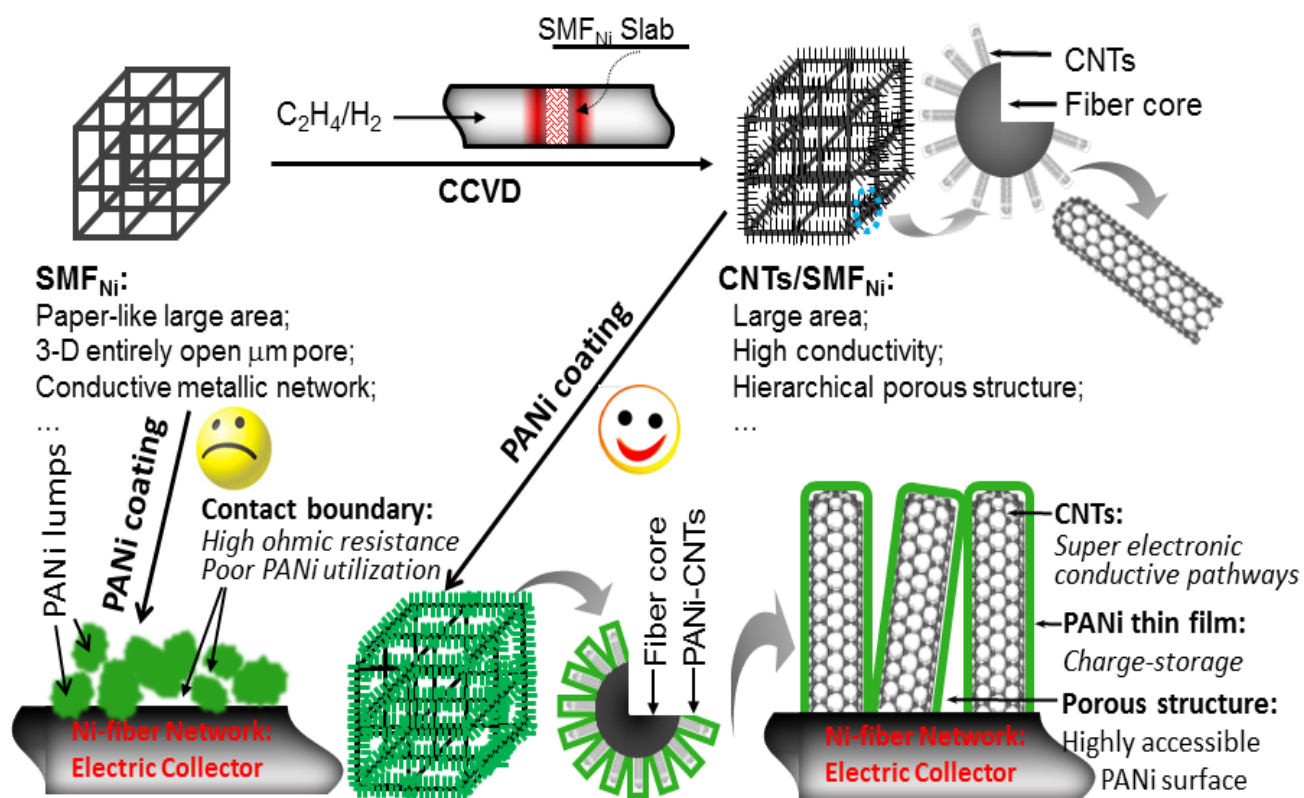
## Experimental Section

*Materials and Fabrication: Thin-sheet CNTs/Ni-fiber preparation.* A circular macroscopic CNTs/Ni-fiber consisting of 38 wt% CNTs was fabricated through CNTs growth on a 3D sinter-locked Ni-fiber slab (80 mm diameter by 0.8 mm thick; consisting of 5 vol% 8 $\mu$ m-Ni-fibers and 95 vol% void volume) by catalytic decomposition of C<sub>2</sub>H<sub>4</sub> in the presence of H<sub>2</sub> at 700 °C, as previously reported elsewhere (F. Jiang, et al., *J. Mater. Chem.*, 2009, **19**, 3632-3637). **PANi-CNTs/Ni-fiber preparation.**

A PANi-sol was obtained by dissolving 100 mg dry PANi-based fine powder (molecule weight: 10000; Alfa Aesar) in 10 mL N-methyl-2-pyrrolidinone (NMP, Alfa Aesar) under vigorously stirring for 1 h at room temperature. The resulted PANi-sol was used to incipiently impregnate the CNTs/Ni-fiber paper. After that, the samples were heated at 100 °C in air for 4 h to completely remove the solvent while leaving PANi thin-film on the CNTs to form uniform PANi-CNTs/Ni-fiber composites. By repeating the above procedure, high PANi content up to 43 wt% in the whole composite could be achieved.

*Characterizations:* The surface morphology and microstructure of the PANi-CNTs/SMF<sub>Ni</sub> composites were examined by means of scanning electron microscopy (SEM, Hitachi S-4800) operating at an accelerating voltage of 3 kV and a transmission electron microscopy (TEM, JEOL-JEM-2010) operating at 200 kV. Fourier transform infrared spectra (FT-IR) were collected on Nicolet Nexus 670 spectrophotometer.

*Electrochemical Property Studies:* Three-electrode system in 1.0 mol L<sup>-1</sup> Na<sub>2</sub>SO<sub>4</sub> aqueous electrolyte (pH = 2.5) was built from the PANi-CNTs/SMF<sub>Ni</sub> hybrids as self-supporting electrodes without any additional binders. Their electrochemical characteristics were obtained by cyclic voltammetry and galvanostatic charge-discharge techniques using a CHI-660C instrument (made in China). Impedance spectroscopy measurements, in the frequency range from 0.1 Hz to 100 kHz, were also performed using the CHI-660C at open circuit voltage of 0.4 V.



**Scheme S1** Concept and procedure for making large-area PANi-CNTs/Ni-fiber hybrid structures. Note: a cubic architecture here is used only to demonstrate the idea and the hybrid actually shows an irregular 3D structure as illustrated by the posterior SEM images.

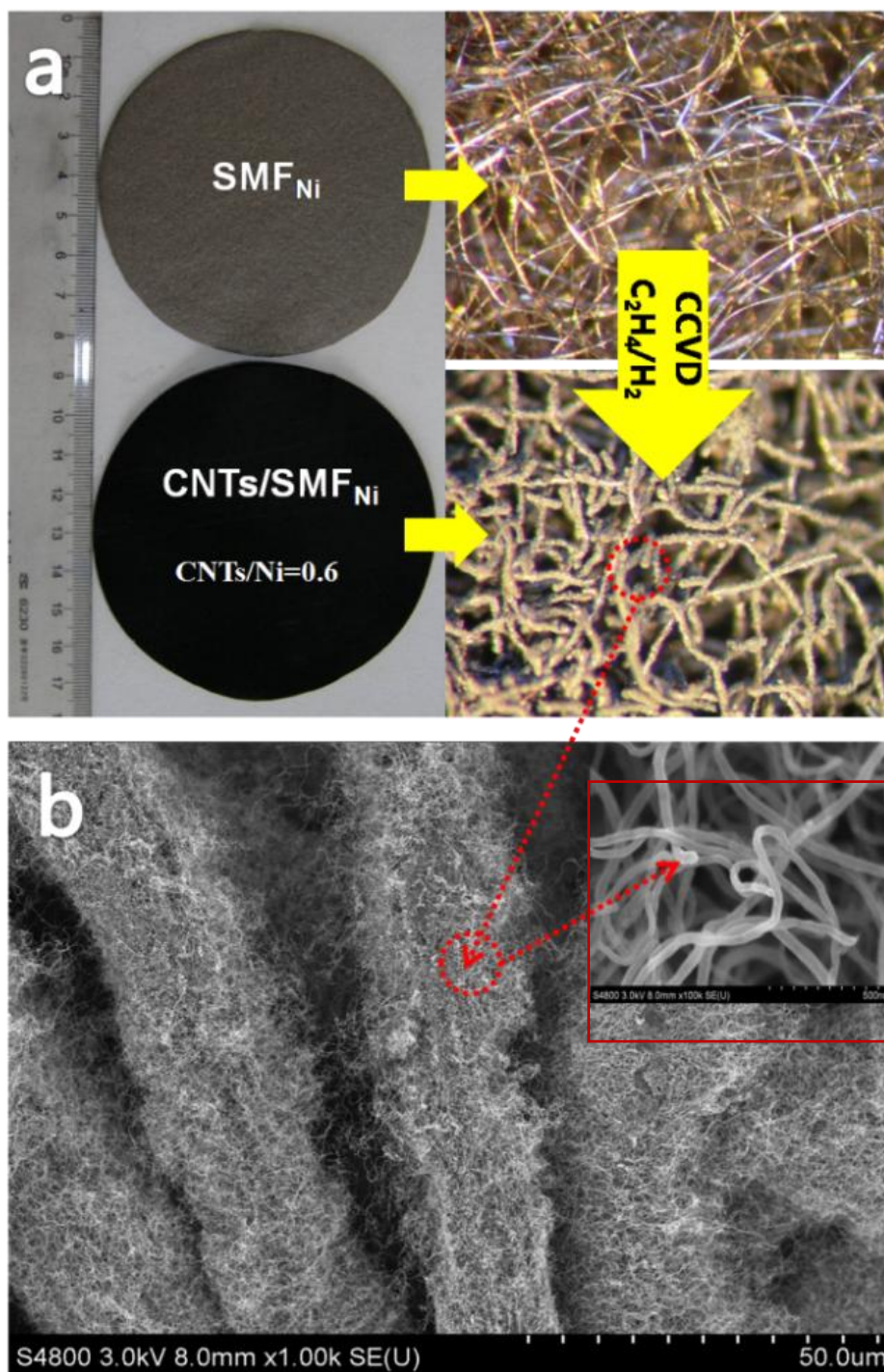


**Fig. S1** (a) Optical photographs of the large-area structure of neat  $SMF_{Ni}$  and  $CNTs/SMF_{Ni}$  composite with 38 wt% CNTs grown on the  $SMF_{Ni}$ ; (b) SEM image of  $CNTs/SMF_{Ni}$  composite.

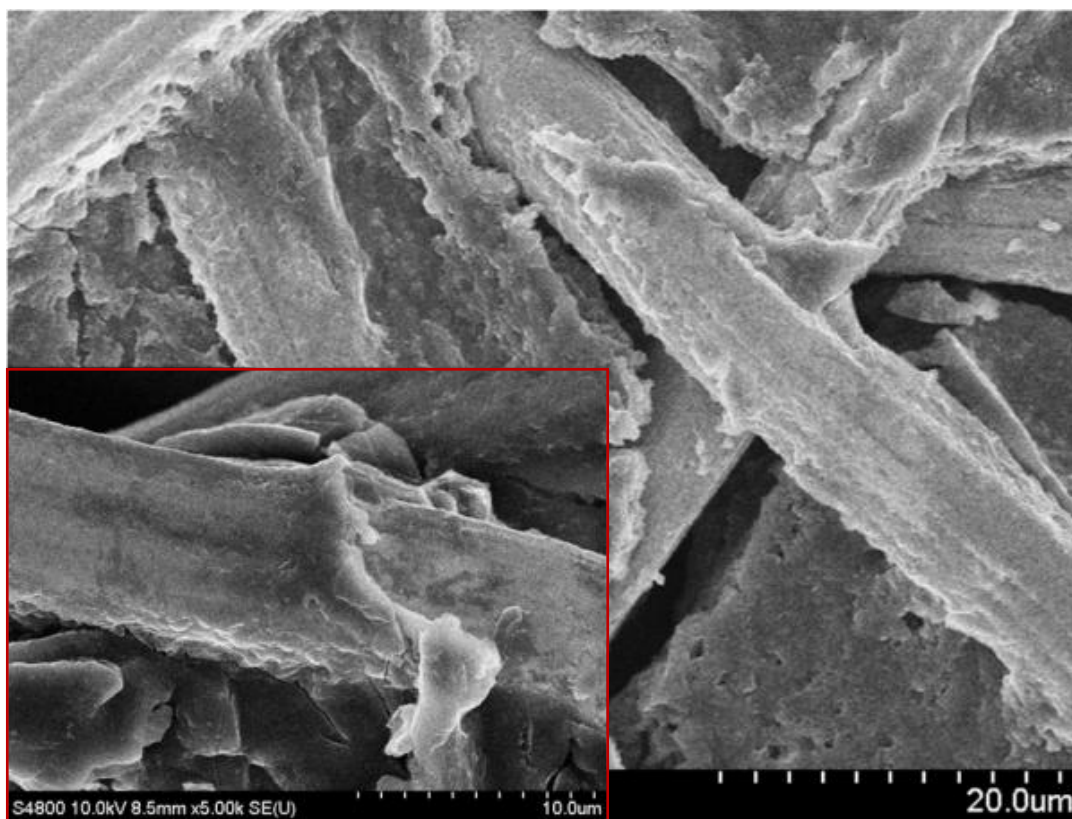


**Fig. S2** SEM images of PANi/SMF<sub>Ni</sub> (~28 wt% PANi) hybrid obtained by PANi-sol coating, showing that PANi preferred to agglomerate between the Ni-fibers rather than cladding along with the fiber of SMF<sub>Ni</sub>.

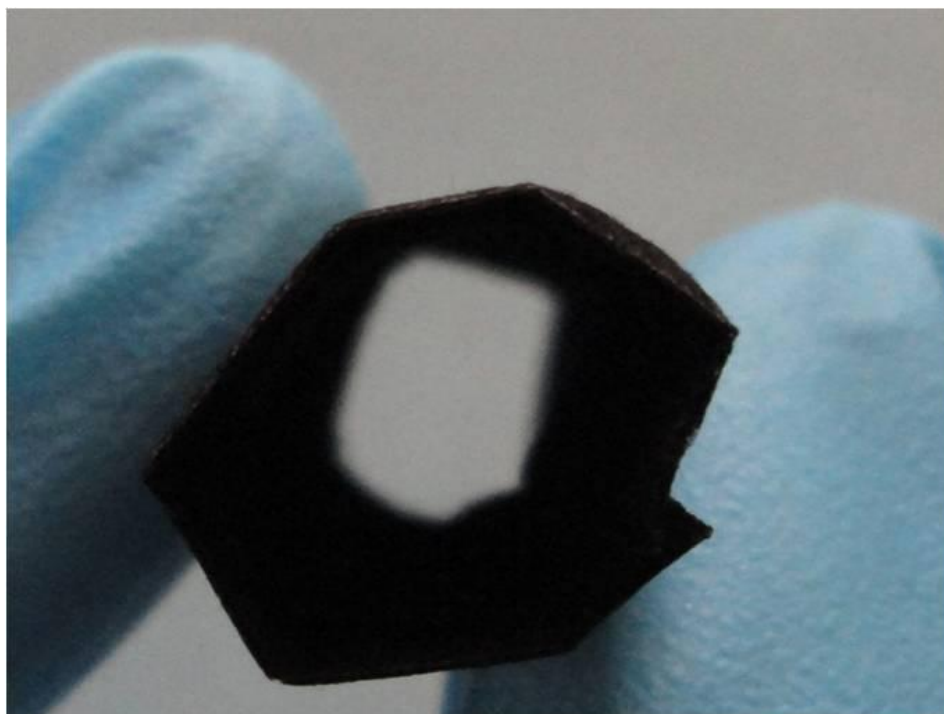


**Fig. S3** Digital photograph of the flexible PANi-CNTs/SMF<sub>Ni</sub> hybrid electrode.

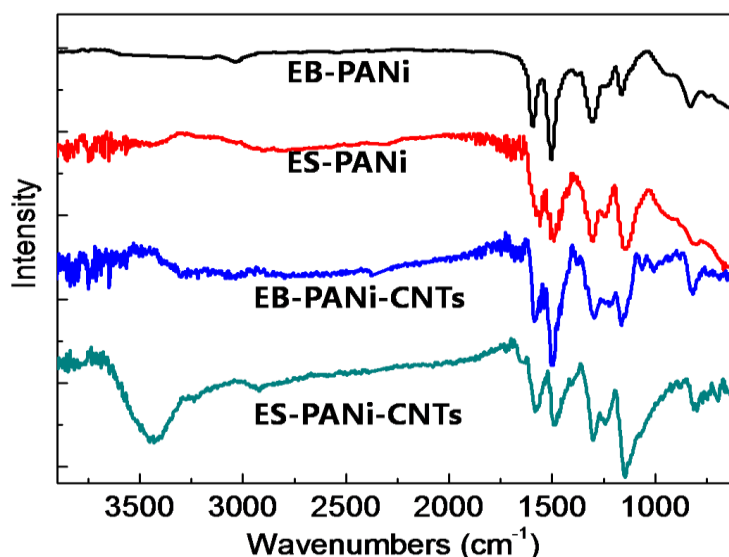


**Fig. S4** FT-IR spectra of EB-PANi, ES-PANi, EB-PANi-CNTs and ES-PANi-CNTs nanocomposites.

Fig. S4 shows the FT-IR spectra of PANi-CNTs nano-composites in the PANi-CNTs/SMF<sub>Ni</sub> hybrids before and after acid treatment. The IR spectra of neat PANi are also collected for reference. Interestingly, all spectra exhibit clear presence of benzenoid ring vibrations at 1497 cm<sup>-1</sup> and quinoidal ring vibrations at 1592 cm<sup>-1</sup>. As well known, the ES-PANi provides a higher signal intensity ratio of quinoidal rings at 1592 cm<sup>-1</sup> to benzenoid rings at 1497 cm<sup>-1</sup> compared to the EB-PANi, due to higher quinoid content as a result of protonization.<sup>S1-S3</sup> In comparison with the pure ES-PANi, the CNTs lead to a further increase of such signal intensity ratio of quinoidal rings to benzenoid rings, indicating that the ES-PANi-CNTs nanocomposites are richer in quinoid units than the pure ES-PANi. This likely suggests that a special interaction took place at the interface between PANi and CNTs thereby promoting and/or stabilizing the quinoidal ring structure. It is noticeable that the IR spectra show clear differences regarding the band centered at 1150 cm<sup>-1</sup> especially an appearance of new band centered at 3400 cm<sup>-1</sup> on the ES-PANi-CNTs nanocomposites. As previously described by MacDiarmid et al.,<sup>S1,S2</sup> the band at 1150 cm<sup>-1</sup>, as the “electronic-like band”, is a characteristic associated with PANi conductivity because it is considered to be a measure of the degree of delocalization of electrons. Both pure ES-PANi and ES-PANi-CNTs nanocomposites deliver strong electronic-like band and therefore are endowed with enhanced conductivity compared to the samples without protonization treatment. By comparison, it is clear that ES-PANi-CNTs nanocomposites offer a more intense electronic-like band than the pure ES-PANi, because of the strong  $\pi$ - $\pi$  interaction between the backbone structure of ES-PANi and CNT surface.<sup>S3,S4</sup> It is not surprising, moreover, that a striking band in N-H stretching region near 3400 cm<sup>-1</sup> appears only on the ES-PANi-CNTs nanocomposites, as a result of promoted “charge-transfer” effect between PANi and CNTs accordingly.<sup>S5</sup>

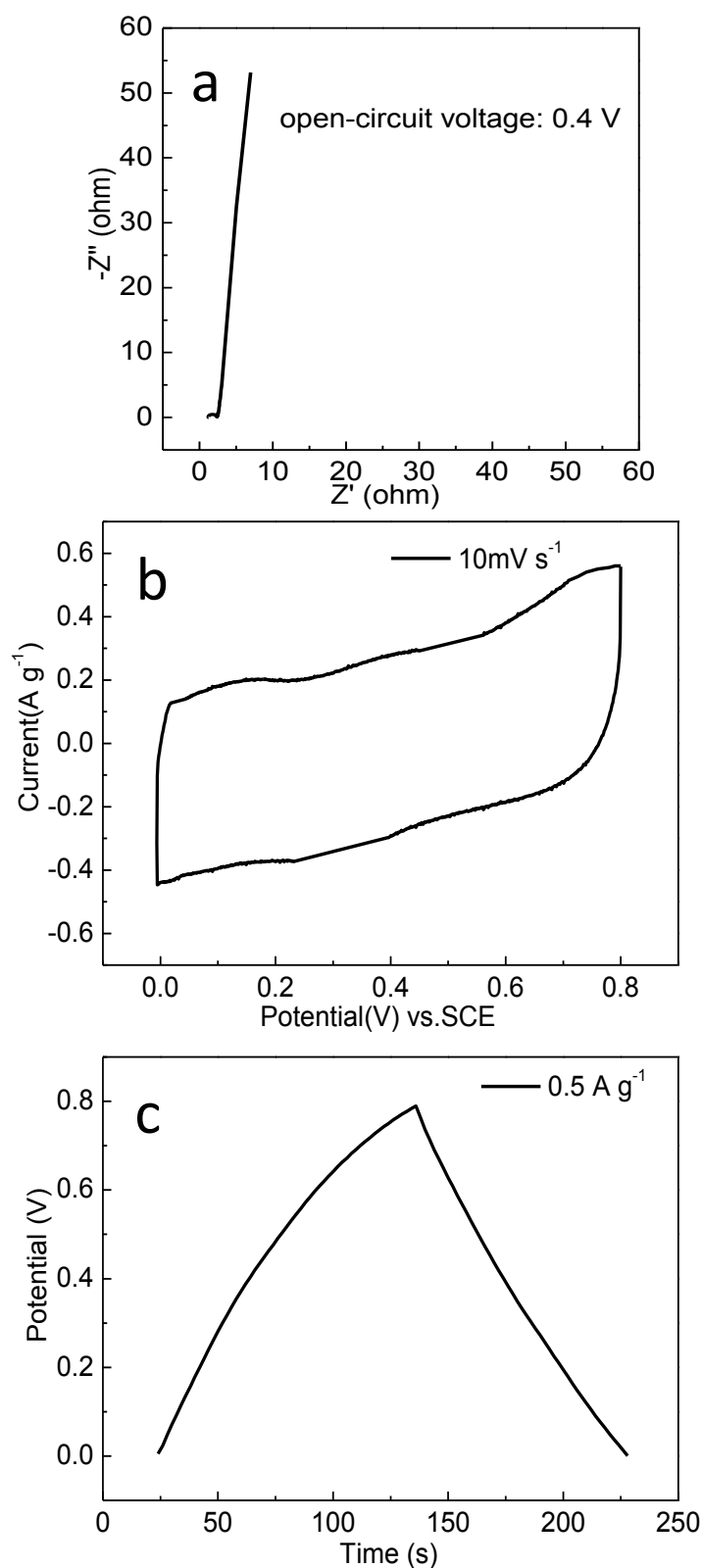


**Fig. S5** Electrochemical properties of CNTs/SMF<sub>Ni</sub> (CNTs: 38 wt%) electrode in 1.0 mol L<sup>-1</sup> Na<sub>2</sub>SO<sub>4</sub> aqueous electrolyte and its SEM images, respectively. (a) impedance spectroscopy (EIS) at an open circuit voltage of 0.4 V; (b) cyclic voltammogram curves at a scan rate of 10 mV s<sup>-1</sup>; (c) charge-discharge curves at a current density of 0.5 A g<sup>-1</sup>.

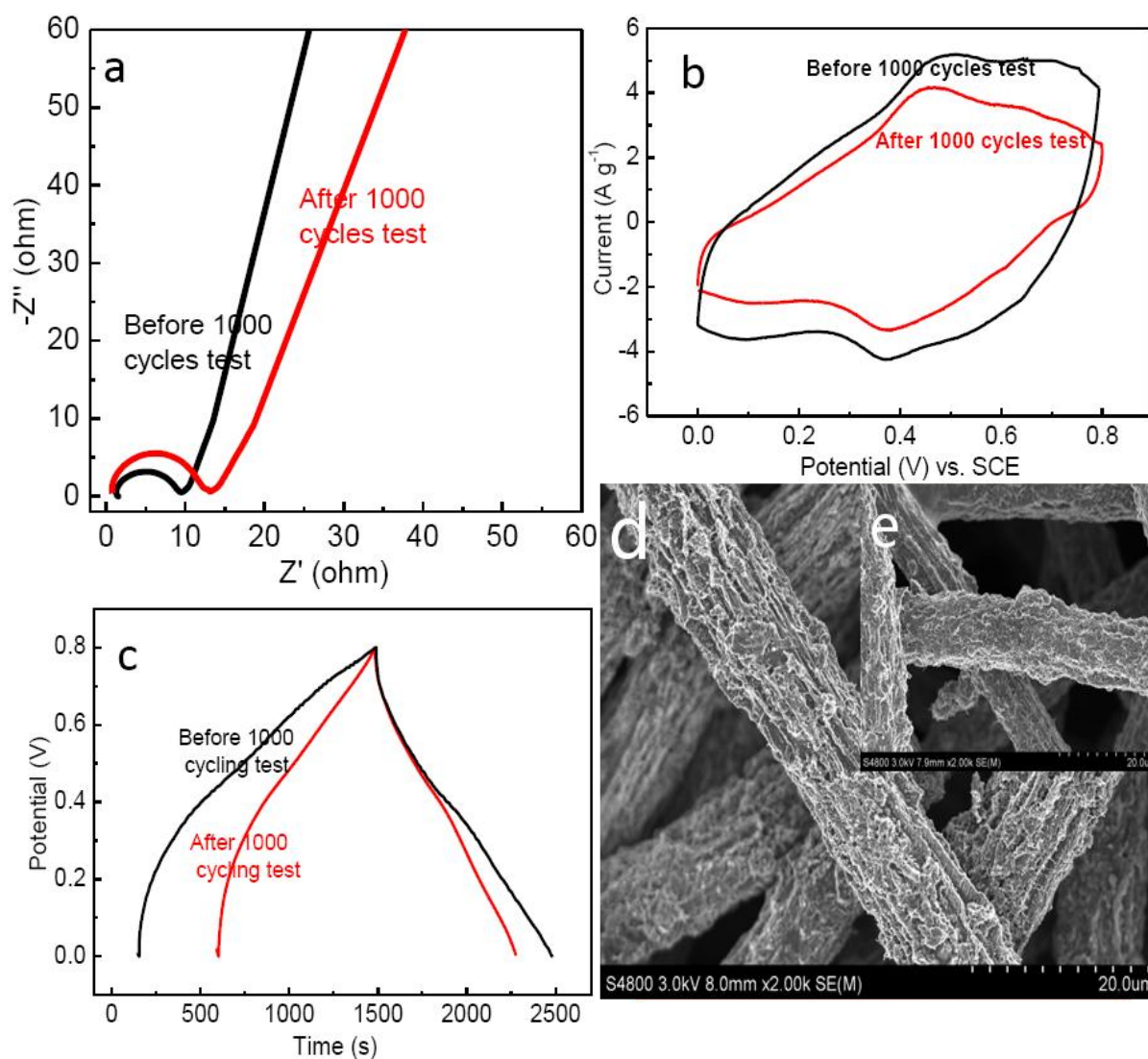
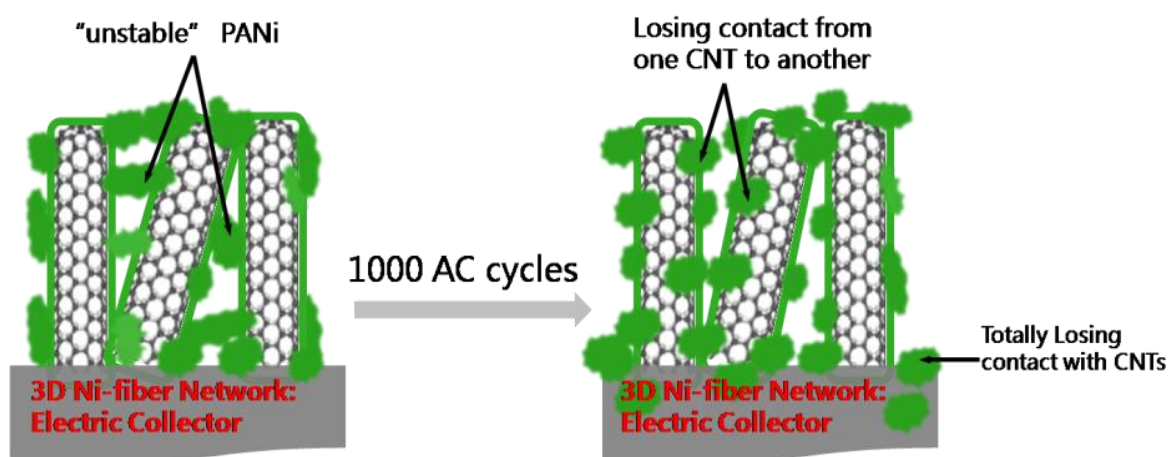


**Fig. S6** Electrochemical properties of PANi-CNTs/SMF<sub>Ni</sub> hybrid electrode before and after 1000 electrochemical cycle testing in 1.0 mol L<sup>-1</sup> Na<sub>2</sub>SO<sub>4</sub> aqueous electrolyte and its SEM images, respectively. (a) impedance spectroscopy (EIS) at an open circuit voltage of 0.4 V; (b) cyclic voltammogram curves at a scan rate of 10 mV s<sup>-1</sup>; (c) charge-discharge curves at a current density of 0.5 A g<sup>-1</sup>; (d,e) SEM images of PANi-CNTs/SMF<sub>Ni</sub> hybrid electrode after 1000 cycles testing.



**Scheme S2** Conjecture of the cause description of capacitance attenuation in 300 charge-discharge cycles. Part of 'unstable' PANi might lose contact from one CNTs to another, some even totally lose contact with CNTs. This absolutely deteriorate the conductivity and reducing the utilization of PANi thereby leading to a capacitance attenuation.

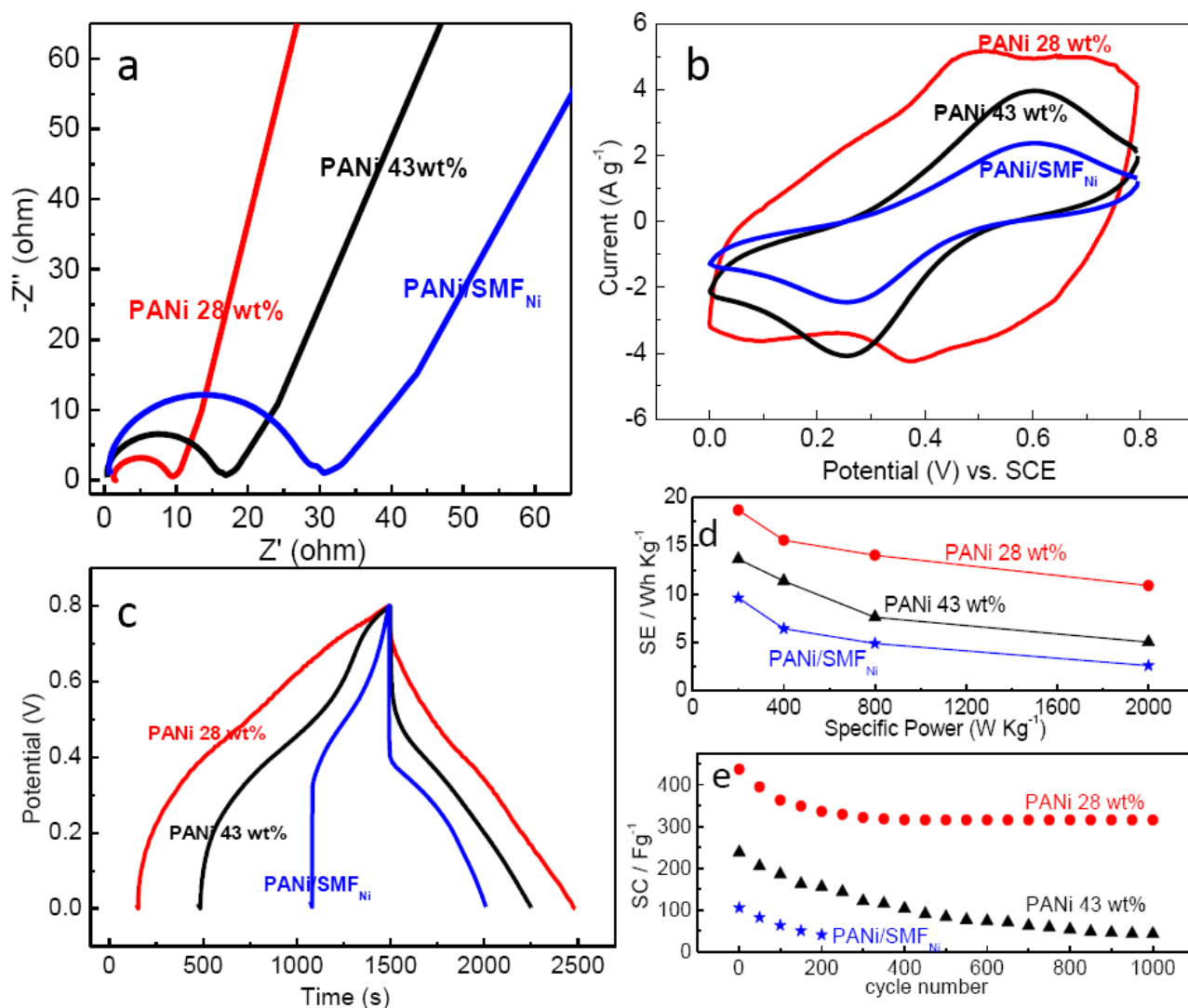


**Fig. S7** Electrochemical testing results of PANi-CNTs/SMF<sub>Ni</sub> hybrid electrode with PANi of 28 wt% and PANi of 43 wt%, and PANi/SMF<sub>Ni</sub> composites (~28 wt% PANi) in 1.0 mol L<sup>-1</sup> Na<sub>2</sub>SO<sub>4</sub> aqueous electrolyte. (a) impedance spectroscopy (EIS) at an open circuit voltage of 0.4 V; (b) cyclic voltammogram curves at a scan rate of 10 mV s<sup>-1</sup>; (c) charge-discharge curves at a current density of 0.5 A g<sup>-1</sup>; (d) energy density vs. specific power, based on total electrode mass including Ni-fiber; (e) cyclability test at a scan rate of 5 A g<sup>-1</sup>.

As we can see, along with the increase of the PANi content in PANi-CNTs/SMF<sub>Ni</sub> hybrid electrodes up to 43 wt%, the electrochemical properties of the hybrid electrodes became similar to those of the PANi/SMF<sub>Ni</sub>, because of the flaws similar to bulk pristine PANi such as mass transportation limitations. Indeed, as shown in **Fig. S8**, lots of PANi lumps were formed for both PANi-CNTs/SMF<sub>Ni</sub> with PANi loading of 43 wt% and PANi/SMF<sub>Ni</sub> samples.

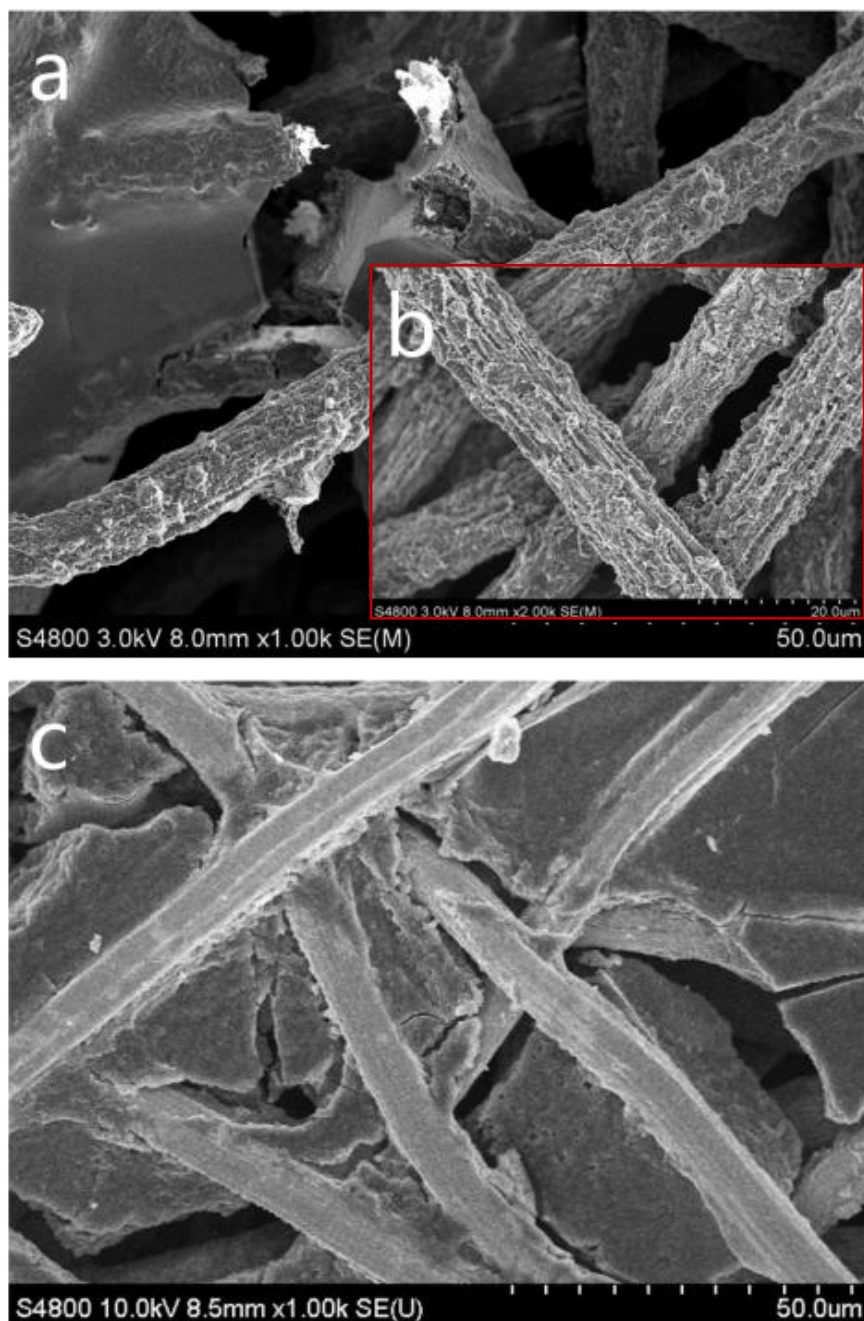


**Fig. S8** SEM images of PANi-CNTs/SMF<sub>Ni</sub> hybrid with PANi content of 43 wt% (a) and 28 wt% (b) as well as SEM image of PANi/SMF<sub>Ni</sub> with PANi of ~28 wt%. Clearly showing that lots of PANi lumps were formed for both PANi-CNTs/SMF<sub>Ni</sub> with PANi loading of 43 wt% and PANi/SMF<sub>Ni</sub> samples.

## References

- S1. S. Quillard, G. Louarn, S. Lefrant, A. G. Macdiarmid, *Phys. Rev. B: Conden. Matter*, 1994, **50**, 12496-12508.
- S2. H. Zengin, W. Zhou, J. Jin, R. Czerw, D. W. Smith, L. Echegoyen, D. L. Carroll, S. H. Foulger, J. Ballato, *Adv. Mater.*, 2002, **14**, 1480-1483.
- S3. R. J. Chen, Y. Zhang, D. Wang, H. Dai, *J. Am. Chem. Soc.*, 2001, **123**, 3838-3839.
- S4. J.-E. Huang, X.-H. Li, J.-C. Xu, H.-L. Li, *Carbon*, 2003, **41**, 2731-2736.
- S5. M. Cochet, W. K. Maser, A. M. Benito, M. A. Callejas, M. T. Martinez, J.-M. Benoit, J. Schreiber, O. Chauvet, *Chem. Commun.*, 2001, 1450-1452